Surface Science 630 (2014) 225–228

Contents lists available at ScienceDirect

Surface Science

journal homepage: www.elsevier.com/locate/susc

Effective mass of a two-dimensional $\sqrt{3} \times \sqrt{3}$ Ga single atomic layer on Si(111)

M. Schnedler [a], Y. Jiang [b], K.H. Wu [c], E.G. Wang [b], R.E. Dunin-Borkowski [a], Ph. Ebert [a,*]

[a] Peter Grünberg Institut, Forschungszentrum Jülich GmbH, 52425 Jülich, Germany
[b] International Center for Quantum Materials, Peking University, Beijing 100871, People's Republic of China
[c] Institute of Physics, Chinese Academy of Sciences, Beijing 100080, People's Republic of China

ARTICLE INFO

Article history:
Received 12 May 2014
Accepted 16 July 2014
Available online 24 July 2014

Keywords:
Effective mass
Scanning tunneling spectroscopy
Surface state

ABSTRACT

The effective mass of the empty conduction band surface state of a single atomic $\sqrt{3} \times \sqrt{3}$ Ga layer on Si(111) is determined using scanning tunneling spectra. The methodology is based on calculating the tunnel current using its dependence on the effective density of state mass and a parabolic band approximation followed by fitting to the measured tunneling spectra. An effective mass of $m_{\mathrm{eff,C}} = 0.59 \pm 0.06$ is obtained, in good agreement with a band structure calculation and inverse photo electron spectroscopy data.

1. Introduction

Future semiconductor devices are likely to rely heavily on nanostructures. Therefore the transport of charge carriers in semiconductor nanostructures is attracting increasing interest. In a semi classical approach, the transport of charge carriers is primarily governed by the effective mass tensor of electrons and holes. Neglecting the crystal anisotropies, the scalar effective mass m^* is reasonably well known for most bulk materials. The effective masses m^* range typically from almost zero [1] to several hundred times the rest electron mass (m_e) [2] in the bulk. However, with ongoing miniaturization of semiconductor devices and the trend towards the use of nanostructures, the increasing surface to volume ratio reduces the relative fraction of bulk material. Hence, transport in semiconductor nanostructures is to a large degree determined by surface and/or interface effects, where little is known about the effective masses.

The knowledge of the dispersion relation $E(k)$ is crucial for the determination of the effective mass. Angle-resolved photoemission spectroscopy (ARPES) delivers information of the momentum and energy, but it is hardly applicable on individual nanostructures. Although scanning tunneling spectroscopy (STS) is ideally suited for probing the local density of states of an individual nanostructure by evaluating the derivative dI/dV of the tunnel current with respect to the tunnel voltage V, it is a very difficult task to quantitatively measure the involved k vectors and hence the dispersion relation. Only in special cases information about the k vectors of the tunneling electrons can be derived from scanning tunneling microscope (STM) measurements: First, one can extract the parallel wave vector $k_\parallel$ of the tunneling electrons from the decay of the local density of states into the vacuum [3–6], since the decay constant κ depends on $k_\parallel$ [7,8]. This method is, however, not yet precise enough to provide quantitative dispersion relations. Second, the wavelength of standing waves present on metallic surfaces is used to derive quantitatively the dispersion relation [9,10]. However, most of the semiconductor surfaces do not exhibit standing electron waves and thus this method is restricted to some special cases.

Therefore, we illustrate here a methodology applicable to individual semiconducting nanostructures for extracting effective masses of a two dimensional $\sqrt{3} \times \sqrt{3}$ Ga single atomic layer on Si(111) from scanning tunneling spectra. The dependence of the tunnel current on the effective density of states mass is utilized to extract the effective mass of empty and filled surface states by fitting calculated to measured tunneling spectra.

2. The effective mass in STS

In order to obtain the effective mass from STS, we recall the relation of the effective mass and the tunnel current: For density of states (DOS) calculations of a d-dimensional system, the effective density of states mass $m_{\mathrm{eff,DOS}}$ is derived from the scalar effective mass of the band $m^* = m_{\mathrm{eff}} \cdot m_e$ using

$$m_{\mathrm{eff,DOS}} = g^{\frac{2}{d}} \cdot m_{\mathrm{eff}}. \quad (1)$$

The degeneracy factor g is the number of equivalent band extrema [11]. The tunnel current can be calculated following the model of Bono and Good [12] applied to semiconductors [8], using a parabolic approximation of the dispersion relation with the effective density of states

* Corresponding author.
E-mail address: p.ebert@fz-juelich.de (P. Ebert).

http://dx.doi.org/10.1016/j.susc.2014.07.024
0039-6028/

mass $m_{\mathrm{eff,DOS}}$. The parabolic approximation is suitable for wave vectors near the valence-band maximum or the conduction-band minimum. The tunnel current between tip and semiconductor is then given by [8,12]:

$$I = \pi R^2 \frac{4\pi e m_e}{h^3}\left(\int_{E_F}^{E_F-eV} dE\ \theta\,(E-\mathrm{EC})^{*}\int_{E}^{e\overline{\Phi}} dW T(W)\right) \quad (2)$$

with the transmission probability $T(W)$

$$T(W) = exp\left(-\sqrt{\frac{8m_e}{\hbar^2}}\int_{z_1}^{z_2}\sqrt{B(z)-W}dz\right). \quad (3)$$

The tunneling area is approximated by Bono and Good with πR^2, where R is the radius of the tip [12]. We use for this 1 nm^2 following Feenstra and Stroscio [8]. E_F and E_C correspond to the Fermi energy and the conduction band edge of the semiconductor, respectively. z_1 (z_2) corresponds to the position of the sample surface (tip). $B(z)$ is the barrier potential in the vacuum gap between the tip and the surface as defined by Ref. [8,12]. $e\overline{\Phi}$ is given by

$$e\overline{\Phi} = \left(1-m_{\mathrm{eff,DOS}}\right)E + m_{\mathrm{eff,DOS}}\cdot E_C. \quad (4)$$

Note that we assume that the tunneling probability is not changed by non-zero parallel wave vectors of the tunneling electrons. At room temperature the momentum transfer can be accommodated by surface phonons. The dispersion of the surface phonon shows branches at low energy (<10 meV) covering all k vectors [13,14]. Hence, the energy loss of the tunneling electrons is negligible compared to the thermal energy resolution at room temperature of ~100 meV. This assumption is supported by the observation of normal tunnel current even for electrons tunneling into or out of states at the edge of the surface Brillouin zone [6].

3. The investigated system

The $\sqrt{3}\times\sqrt{3}$ Ga overlayer on a Si(111) was prepared by evaporating approximately 0.33 monolayers of Ga on a previously cleaned and degassed 7×7 reconstructed Si(111) surface at ~750 K, followed by a slow cool down to room temperature [15]. The STM measurements were performed at room temperature using electrochemically etched tungsten tips.

The geometrical structure of the $\sqrt{3}\times\sqrt{3}$ Ga overlayer on Si(111), illustrated in Fig. 1a and b, is analogous to that of the $\sqrt{3}\times\sqrt{3}$ Al on Si(111) calculated by Northrup [16]: The Ga adatoms are located at so-called T_4 sites centered above three Si atoms in the uppermost substrate layer. The bond length between the adatoms and the substrate Si atoms is 2.5 Å [16]. The Ga adatoms cause a downward displacement of the first and second layer Si atoms by 0.0265 Å and 0.334 Å, respectively [16]. Taking into account these displacements, one can derive the distance perpendicular to the surface between the Ga adatoms and the first layer of Si substrate atoms to be $\Delta_{12} = 1.363$ Å(Fig. 1b).

4. Experimental results

Fig. 1(c) shows a filled state STM image of the $\sqrt{3}\times\sqrt{3}$ Ga overlayer on the Si(111) substrate. Each maximum corresponds to one Ga or Si adatom [15]. The brighter maxima arise from Si adatoms at $\sqrt{3}\times\sqrt{3}$ adatom sites [17], acting as dopants [15]. At negative voltage their localized state in the band gap contributes to a locally higher tunnel current, which leads to the difference in brightness compared to the Ga atoms: Fig. 2 shows atomically resolved tunneling spectra measured above Ga (filled blue squares) and Si atoms (red filled circles). The Si adatoms exhibit a pronounced localized state in the gap at negative voltages. The resulting tunnel current is one to two orders of magnitudes larger above Si adatoms than above Ga adatoms.

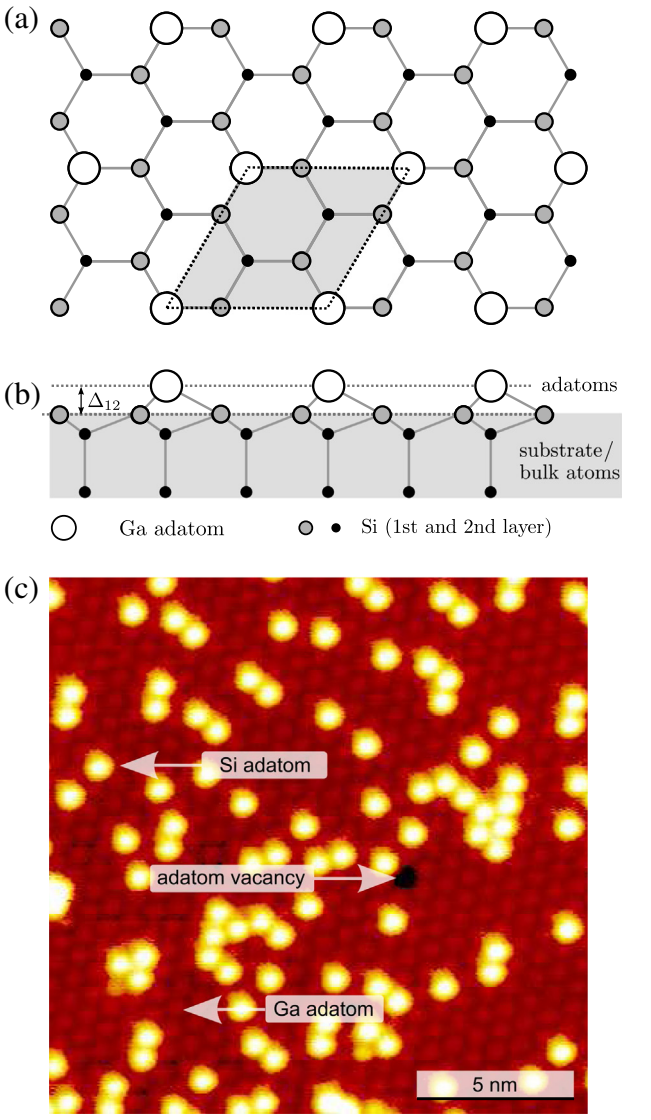

Fig. 1. (a) Schematic top view of the $\sqrt{3}\times\sqrt{3}$ Ga–Si(111) structure. The unit cell of the Ga overlayer is indicated by the gray shaded area. (b) Side view. The gray shaded area marks the substrate. The distance perpendicular to the surface between the Ga adatoms and the first layer of Si substrate atoms is given by Δ_{12}. (c) Constant-current STM image of the filled states of the $\sqrt{3}\times\sqrt{3}$ Ga–Si(111) structure measured at −2.0 V. Bright spots represent Si adatoms on $\sqrt{3}\times\sqrt{3}$ Ga sites.

Since the tip is not perfectly point-shaped, the $I(V)$ spectra obtained above Ga adatoms are also slightly influenced by the localized Si states in the band gap region. This shows up as a slight increase of the tunnel current at negative voltages, near the valence band edge, as can be seen in Fig. 2. Subtracting this background (solid gray line) the pure valence band current is obtained (I_V). The resulting band gap agrees well with that of Si. Due to the presence of the filled gap state at Si adatoms, we concentrate here on the empty conduction band states at Ga sites only, where the influence of the Si adatoms can be neglected. In order to minimize the influence of the Si adatoms on the tunnel current further, no tunneling spectra from Ga sites with nearest neighbor Si adatoms were used. This allows to reduce the influence of the Si adatoms by about 2 orders of magnitude, since the gap state of the Si adatoms is spatially highly localized [6]. Such tunneling spectra, acquired above many Ga adatom sites, were selected and averaged.

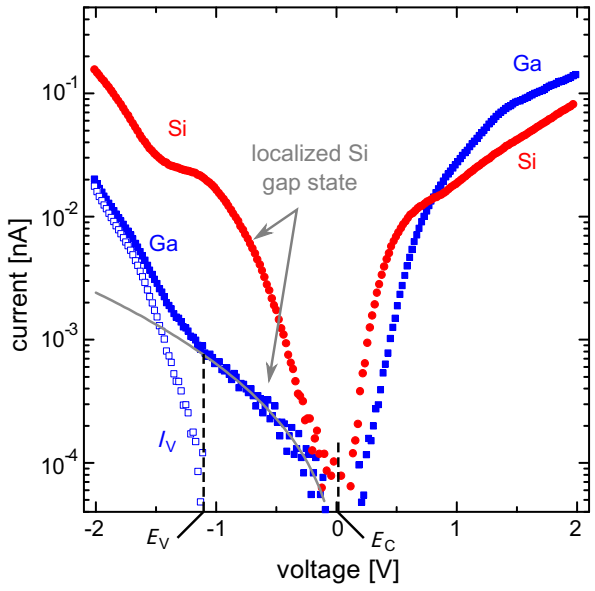

Fig. 2. Averaged $I(V)$ tunneling spectra taken above Ga (filled blue squares) and Si (filled red circles) adatoms. The tunneling spectra above the Ga adatoms exhibit a background within the band gap due to localized Si states. The background (gray fitted curve) has been subtracted to obtain the pure valence band current shown as blue empty squares (I_V). The tip-sample separation is identical all curves. (For interpretation of the references to color in this figure legend, the reader is referred to the web version of this article.)

5. Determination of the effective electron mass

The tunnel current approximation given by Eq. (2) assumes that the tip-induced band bending shifting the band edges is negligible. In the present case, the extremely high two-dimensional Si concentration of about 20%, acting as donors, leads to a very small screening length of less than 0.5 nm [15]. Hence, the electric field between the tip and the sample does not penetrate into the semiconductor and one can neglect the tip-induced band bending [15,18].

Without tip-induced band bending, two components contribute to the tunnel current at positive voltages (empty states): Electrons can tunnel into bulk states of the Si substrate and into the states of the $\sqrt{3} \times \sqrt{3}$ Ga adatom layer [6]. The energy bands of bulk and surface states exhibit different band edges. The conduction band edge of the Ga overlayer, $E_{C,surface}$, was determined from measurements of the decay constant κ [6] and a band structure calculation of the $\sqrt{3} \times \sqrt{3}$ Ga layer [19]. The bulk conduction band edge $E_{C,bulk}$ was taken from the measurement of the position of the Fermi energy relative to the conduction band edge on this system [15]. Hence, the band edges, relative to the Fermi energy are

$$\begin{aligned} E_{C,surface} &= 0.27\,eV \\ E_{C,bulk} &= 0.013\,eV. \end{aligned} \tag{5}$$

Thus, at small positive voltages, electrons tunnel from the tip into empty Si substrate (bulk) states below the Ga adatom layer first. Then at larger positive voltage, electrons start to tunnel into the empty dangling bond states above the Ga adatoms, too. Since the surface states (dangling bonds of the Ga adatoms) are physically closer to the tip than the Si substrate (bulk) states, the former dominate the tunnel current at larger voltages [6]. Hence two different effective tip-sample separations need to be taken into account in the data analysis. The difference in the tip-sample separation was estimated using the distance between the Ga adatoms and the first layer of Si atoms in the substrate (Δ_{12} =1.363 Å) (Fig. 1b).

Tunneling spectra were acquired at 6 different tip-sample separations z changed in steps of 0.2 Å (i.e. $z = z_0 + \Delta z$, with $\Delta z = n \cdot 0.2$ Å). Since the absolute tip-sample separation is not measurable by STM, z_0 was used as fitting parameter to fit simultaneously all 6 data sets. Using Eqs. (2)–(4) the tunnel current component into the Si substrate (bulk) was calculated with a fitted z using the bulk effective mass of a Si(111) plane [11]. Then the Ga adatom (surface) component was computed using a reduced tip-sample separation, due to the smaller distance of the tip to the Ga adatoms than to the Si substrate atoms. The total calculated tunnel current was then fitted to the $I(V)$ spectra taken above Ga adatoms by varying $m_{eff,DOS}$ of the surface state.

For the fits we used a work function for the W tip of 4.5 eV, a smallest tip-sample (bulk plane) separation z_0 = 1.195 nm as defined above for all tunneling spectra offsetted by multiples of 0.2 Å, and a tunneling area of 1 nm^2. Note that the parameters are not fully independent in the calculation: If one assumes a larger (smaller) tunneling area, the tunnel current increases (decreases) proportionally (i.e., not changing the slope of the logarithmic tunnel current in Fig. 3). This increase (decrease) can be directly compensated by a larger (smaller) tip-sample separation (also not changing the slope of the logarithmic tunnel current). Similarly, a smaller (larger) tip work function increases (decreases) the tunnel current (through changing the barrier potential $B(z)$), which again can be compensated by a larger (smaller) tip-sample separation. Since the tip-sample separation z_0 is used as fit parameter besides the effective mass, the result does not depend on the exact values of the tunneling area and tip work function. Therefore, we assumed the work function and tunneling area in analogy to Feenstra and Stroscio [8]. Finally, due to the absence of tip-induced band bending the tip radius is not affecting the electrostatics of the tip-sample system and hence we can use a one dimensional calculation of the tunnel current.

Fig. 3 shows an example of the calculated tunnel current (red curve) fitted to the spectra measured above the Ga atoms (black dots) at positive voltages. At voltages smaller than +0.27 V only the bulk states of the uppermost Si substrate layer contribute to the tunnel current, since no surface states are available in this energy range (within the surface band gap). Above +0.27 V the surface conduction band states lead to a significant increase in tunnel current, resulting in a discontinuity in the slope. For voltages smaller than +0.5 V the simulated tunnel

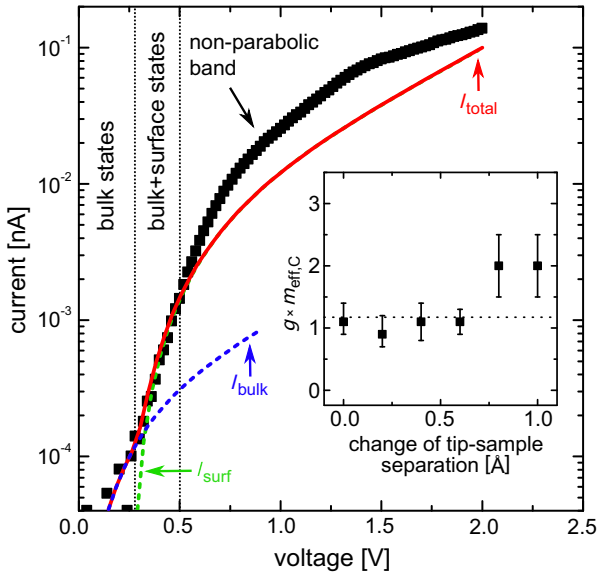

Fig. 3. Comparison of the calculated total tunnel current (red curve, I_{total}), the calculated tunnel current into empty bulk states (I_{bulk}), and the calculated tunnel current into the empty states of the surface adatom layer (I_{surf}) with the tunnel current measured above the Ga atoms (black dots) at positive voltages. Inset: Effective-DOS mass of the surface conduction band states obtained from the fits of the calculated current to the measured tunnel current versus the change of the tip-sample separation (relative to a tip-sample separation fixed at +0.8 V and 20 pA). The dotted line shows the weighted average of the effective-DOS mass.

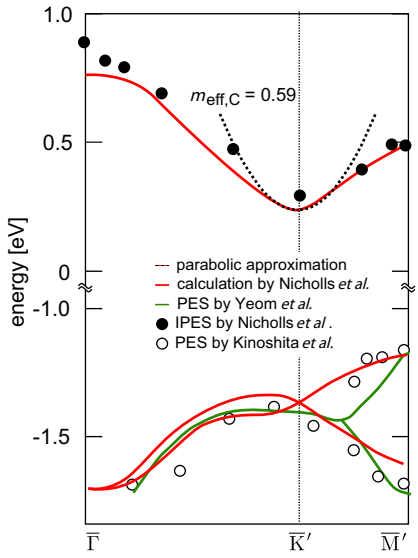

Fig. 4. Dispersion of the valence- and conduction band of a $\sqrt{3} \times \sqrt{3}$ Ga overlayer on Si(111): band structure calculations (red curve) and inverse angle-resolved photo electron spectroscopy (IPES) data (filled circles) of Nicholls et al. [19], as well as angle-resolved photo electron spectroscopy (PES) data taken from Kinoshita et al. [21] (open circles) and Yeom et al. [22] (green curve). The energy is given relative to the Fermi energy as measured on *n*-type Si(111) substrates [15]. The PES data on *n*-type Si(111) is hence not shifted, whereas the IPES on a *p*-type substrate and to this data adjusted theoretical band structure were shifted downward to match the measured surface conduction band onsets. In addition the underestimation of the band gap in DFT calculations was corrected [19]. The dashed parabolas represent the parabolic approximation calculated from the measured effective mass $m_{eff,C} = 0.59$ for the conduction band minimum. (For interpretation of the references to color in this figure legend, the reader is referred to the web version of this article.)

current is in good agreement with the measured spectrum. When the voltage exceeds +0.5 V the measured tunnel current increases faster than the computed one. This phenomenon is attributed to the non-parabolic flattening of the dispersion of the empty surface state above +0.5 eV as illustrated in Fig. 4, resulting in a higher density of states than in the parabolic approximation.

The fit of the conduction band tunnel current was repeated for different tip-sample separations and the effective-DOS mass shown in the inset of Fig. 3 were deduced. Two data points in the inset in Fig. 3 exhibit a higher effective mass and a larger error, due to the poorer signal-to-noise ratio at larger tip-sample separations. With the degeneracy factor of the surface conduction band minimum at the $\overline{K}'$ point of $g = 2$ and Eq. (1), we derive an average effective mass of the surface conduction band state of $m_{eff,C} = 0.59 \pm 0.06$ from $m_{eff,DOS}$. The parabolic dispersion relation $E(k) = \hbar^2 k^2/(2m_{eff,C}m_e)$ was plotted as dotted line in Fig. 4 using the determined value of $m_{eff,C}$. A good agreement with the band structure calculation and the inverse angle resolved photoelectron spectroscopy (IPES) data [19] is found for energies near the surface conduction band minimum. At an energy of approximately 0.2 eV above the surface conduction band minimum (corresponding to ≈0.5 V in Fig. 3), the parabolic approximation deviates increasingly from the calculated dispersion relation. Other calculations yield the same band structure [20].

6. Conclusions

A methodology for the determination of the effective masses of surface states from scanning tunneling spectra is demonstrated using single atomic $\sqrt{3} \times \sqrt{3}$ Ga layers on Si(111) as model system. The effective mass of the empty surface states was determined by fitting the calculated tunnel current to the measured one. For the empty state in the conduction band an effective mass of $m_{eff,C} = 0.59 \pm 0.06$ was obtained in good agreement with a band structure calculation and inverse photo electron spectroscopy data. The methodology demonstrated here can be applied on any surface or nanostructure, even in the absence of surface charge density waves, as it is based only on the dependence of the tunnel current on the effective density of states mass.

Acknowledgments

The authors thank the National Basic Research Programs of China and the National Science Foundation of China for financial support.

References

[1] K.S. Novoselov, A.K. Geim, S.V. Morozov, D. Jiang, M.I. Katsnelson, I.V. Grigorieva, S.V. Dubonos, A.A. Firsov, Nature 438 (2005) 197.
[2] C. Broholm, G. Aeppli, R.N. Kleiman, D.R. Harshman, D.J. Bishop, E. Bucher, D.L. Williams, E.J. Ansaldo, R.H. Heffner, Phys. Rev. Lett. 65 (1990) 2062.
[3] J.A. Stroscio, R.M. Feenstra, A.P. Fein, Phys. Rev. Lett. 57 (1986) 2579.
[4] R.M. Feenstra, A. Stroscio, A.P. Fein, Surf. Sci. 181 (1987) 295.
[5] L. Ivanova, S. Borisova, H. Eisele, M. Dähne, A. Laubsch, Ph. Ebert, Appl. Phys. Lett. 93 (2008) 192110.
[6] Ph. Ebert, S. Landrock, Y. Jiang, K.H. Wu, E.G. Wang, R.E. Dunin-Borkowski, Nano Lett. 12 (2012) 5845.
[7] J. Tersoff, D.R. Hamann, Phys. Rev. Lett. 50 (1983) 1998.
[8] R.M. Feenstra, J.A. Stroscio, J. Vac. Sci. Technol. B 5 (1987) 923.
[9] J.E. Ortega, F.J. Himpsel, G.J. Mankey, R.F. Willis, Phys. Rev. B 47 (1993) 1540.
[10] C.S. Jiang, H.B. Yu, X.D. Wang, C.K. Shih, P. Ebert, Phys. Rev. B 64 (2001) 235410.
[11] F. Stern, W.E. Howard, Phys. Rev. 163 (1967) 816.
[12] J. Bono, J.R.H. Good, Surf. Sci. 175 (1986) 415.
[13] J. Fritsch, U. Schröder, Phys. Rep. 309 (1999) 209.
[14] J. Schmidt, H. Ibach, J.E. Müller, Phys. Rev. B 51 (1995) 5233.
[15] S. Landrock, Y. Jiang, K.H. Wu, E.G. Wang, K. Urban, Ph. Ebert, Appl. Phys. Lett. 95 (2009) 072107.
[16] J.E. Northrup, Phys. Rev. Lett. 53 (1984) 683.
[17] R.J. Hamers, J.E. Demuth, Phys. Rev. Lett. 60 (1988) 2527.
[18] A. Laubsch, K. Urban, Ph. Ebert, Phys. Rev. B 80 (2009) 245314.
[19] J.M. Nicholls, B. Reihl, J.E. Northrup, Phys. Rev. B 35 (1987) 4137.
[20] U. Grossner, J. Furthmüller, F. Bechstedt, Phys. Rev. B 64 (2001) 165308.
[21] T. Kinoshita, S. Kono, T. Sagawa, Solid State Commun. 56 (1985) 681.
[22] H.W. Yeom, K. Yoo, D.-H. Oh, Surf. Sci. 605 (2011) 146.